PROCEEDINGS OF SCIENCE

Radion Portal Dark Matter in Stabilized Warped Extra-Dimensions

R. Sekhar Chivukula,[a] **Joshua A. Gill,**[d] **Kenn S. Goh,**[b,*] **Kirtimaan A. Mohan,**[c] **George Sanamyan,**[b] **Dipan Sengupta,**[d] **Elizabeth H. Simmons**[a] **and Xing Wang**[a,e]

[a] *Department of Physics and Astronomy, University of California, San Diego, 9500 Gilman Drive, La Jolla, CA-92093, USA*

[b] *ARC Centre of Excellence for Dark Matter Particle Physics, Department of Physics, University of Adelaide, South Australia 5005, Australia*

[c] *Department of Physics and Astronomy, Michigan State University 567 Wilson Road, East Lansing, MI-48824, USA*

[d] *Sydney Consortium for Particle Physics and Cosmology, School of Physics, The University of New South Wales, Sydney NSW 2052, Australia*

[e] *Dipartimento di Matematica e Fisica, Università degli studi Roma Tre, Via della Vasca Navale 84, I-00146, Rome, Italy*

E-mail: rschivukula@physics.ucsd.edu, joshua.gill@unsw.edu.au, kennshern.goh@adelaide.edu.au, kamohan@msu.edu, george.sanamyan@adelaide.edu.au, dipan.sengupta@unsw.edu.au, ehsimmons@UCSD.EDU, xingwang1990@gmail.com

We analyze dark matter (DM) annihilation in a stabilised Randall-Sundrum (RS) model, where the radion—the lightest spin-0 Kaluza-Klein state—acts as a portal between DM and the Standard Model (SM). By recasting limits from axion-diphoton couplings and collider searches for spin-0 resonances, we constrain the radion's parameter space and demonstrate that weakly interacting massive particles (WIMPs) in the 100–500 GeV mass range can satisfy the observed relic abundance while evading direct detection and collider bounds. Furthermore, the theoretical framework of RS models mandates a sub-TeV radion mass, ergo distinguishing it from ad-hoc dilaton portals where the radion mass is a free parameter.

The European Physical Society Conference on High Energy Physics (EPS-HEP2025)
7-11 July 2025
Marseille, France

*Speaker

 ISSN 1824-8039 . Published by SISSA Medialab.

PoS(EPS-HEP2025)042

1. Introduction

The dark matter (DM) problem is established through gravitational evidence from galaxies, clusters, and the cosmic microwave background (CMB) [1–3]. Thermal weakly interacting massive particles (WIMPs) naturally reproduce the observed relic abundance via freeze-out [4], but null direct-detection results now exclude large regions of the GeV–TeV mass range [5]. Theories of warped extra dimensions [6–9] provide an alternative origin for the weak scale and a natural home for WIMPs. In this contribution, we investigate the Randall–Sundrum model (RS1), where the 4D world is a slice of AdS_5 bounded by the ultraviolet (UV, Planck-scale) brane and the infrared (IR, TeV-scale) brane; IR-localized fields couple to gravity-sector excitations with strength set by an effective scale Λ_π. Imposing a stabilization mechanism on the RS background [10–12] introduces a bulk scalar $\hat{\phi}$ and a physical scalar fluctuation—the *radion* $\hat{r}$, the latter being the lightest excitation of the gravitational sector. In this contribution, we show that the radion provides a resonant portal between IR-brane DM and the Standard Model (SM), whilst accounting for a proper treatment of metric background deformations ("back-reaction"). The viable freeze-out regime occurs for $\Lambda_\pi \sim$ 20–100 TeV with m_r below the TeV scale. The leading discovery handle in the remaining parameter space is the spin-2 Kaluza-Klein (KK) sector.

2. Model and background

The gravitational action is detailed in [13–16], but the upshot is that it includes a 5D Einstein-Hilbert term, as well as a bulk scalar field $\hat{\phi}$ equipped with a scalar potential

$$V_{\hat{\phi}} = \frac{1}{2}\sqrt{-G}G^{MN}\partial_M\hat{\phi}\partial_N\hat{\phi} - \left[\sqrt{-G}V(\hat{\phi}) + \sum_{i=1,2}\sqrt{-\bar{G}}\,V_i(\hat{\phi})\delta(y_i)\right] \tag{1}$$

where G_{MN} is the 5D metric (with inverse G^{MN} and determinant G), $\hat{\phi}$ is a bulk scalar field, and $V(\hat{\phi})$ is its bulk potential. The quantities $\bar{G}_{\mu\nu}$ and $\bar{G}$ denote the induced 4D metric and its determinant on branes located at $y = y_i$. The terms proportional to $\delta(y - y_i)$ are the brane-localized potentials $V_i(\hat{\phi})$, with $y_1 = 0$ and $y_2 = \pi r_c$ (equivalently $\varphi = 0, \pi$). The boundary potentials are chosen such that the background geometry is stabilized[10, 11]. We parameterize the 5D metric of our stabilized RS setup following [15–17] :

$$G_{MN} = \begin{pmatrix} e^{-(2A(\varphi)+\hat{u})}g_{\mu\nu} & 0 \\ 0 & -r_c^2(1+2\hat{u})^2 \end{pmatrix} \tag{2}$$

in terms of coordinates $x^M := (x^\mu, \varphi)$ with $0 \le \varphi \le \pi$, corresponding to the orbifold $S^1/\mathbb{Z}_2$. The UV and IR branes sit at the endpoints $\varphi = 0$ and $\varphi = \pi$ (equivalently $y = 0$ and $y = \pi r_c$). Here $A(\varphi)$ is the warp factor and r_c encodes the inter-brane separation. The auxiliary field

$$\hat{u} := \frac{e^{2A(\varphi)}}{2\sqrt{6}}\,\kappa\,\hat{r}(x,\varphi), \tag{3}$$

where $\kappa \equiv (4/M_5^3)^{1/2}$ for the 5D Planck constant M_5. Fluctuations over the flat 4D background $\eta_{\mu\nu}$ (in the "mostly-minus" convention) are expressed as

$$g_{\mu\nu} := \eta_{\mu\nu} + \kappa\hat{h}_{\mu\nu}(x_\mu, y)\,, \tag{4}$$

for metric fluctuations $\hat{h}_{\mu\nu}(x, y)$.

The tensor and scalar fluctuations are respectively expressed as KK towers of states

$$\hat{h}_{\mu\nu}(x, \varphi) = \frac{1}{\sqrt{r_c}} \sum_{n=0}^{+\infty} \hat{h}^{(n)}_{\mu\nu}(x)\, \psi_n(\varphi), \tag{5}$$

$$\hat{r}(x, \varphi) = \frac{1}{\sqrt{r_c}} \sum_{i=0}^{+\infty} \hat{r}^{(i)}(x)\, \gamma_i(\varphi), \tag{6}$$

with ψ_n and γ_i forming orthogonalising basis functions for either sectors. For the spin-2 sector, the $n = 0$ mode represents the massless graviton that propagates Einstein's general relativity in four space-time dimensions, and $n \geq 1$ states corresponding to massive KK graviton excitations. Analogously, the $i = 0$ mode of the scalar sector corresponds to the radion, with further $i \geq 1$ modes named Goldberger-Wise (GW) scalar states [10, 11].

Furthermore, we follow [15, 16] and employ the superpotential inspired DeWolfe-Freedman-Gubser-Karch (DFGK) model [12] for the scalar sector, obtaining the following analytic solutions to the background equations:

$$\phi_0(\varphi) = \phi_1 e^{-ur_c|\varphi|}\,, \tag{7}$$

$$A(\varphi) = kr_c|\varphi| - \frac{1}{48}\phi_1^2\left[1 - e^{-2ur_c|\varphi|}\right]\,, \tag{8}$$

where $\phi_1 = \phi(0)$ is the value of the scalar field on the Planck brane and the parameter

$$u = \frac{1}{\pi r_c} \log \frac{\phi_1}{\phi_2} \tag{9}$$

encoding the variation along the extra dimension, where $\phi_2 = \phi(\pi)$ is the value of the scalar field on the TeV brane. Requiring the hierarchy (set by k) to be large, Further details regarding the procedure to obtain said spectrum and computation of couplings, as well as self-interactions among the matter and the gravitational sector can be found in [15, 16, 18].

3. Experimental constraints and back-reaction phenomenology

Phenomenologically, it is convenient to trade the input parameters of the model $\{r_c, k, u, \phi_1\}$ — or equivalently the dimensionless combinations $\{kr_c, ur_c, \phi_1\}$ — for the physical set $\{\Lambda_\pi, m_1, m_r\}$[1], where Λ_π is the cutoff scale which determines the couplings of the KK modes, m_1 is the lightest spin-2 KK mass and $m_r = m_{(0)}$ is the lightest spin-0 KK mass (radion mass). With these parameters, it has been shown that diphoton searches [21] constrain the lightest spin-2 mass to be $m_1 \geq 4$ TeV for a cutoff scale $\Lambda_\pi \geq 20$ GeV[2] [18]. In addition to existing diphoton searches from Belle-II, ATLAS and CMS [20–24], we may recast existing constraints on the diphoton coupling of axion-like particles (ALP) (see Figure 1 for compilation of these constraints on the $\Lambda_\pi - m_r$ plane). We

[1] The fourth parameter would be the mass of the lightest GW scalar, $m_{(1)}$. However, in this regime we have maximised the allowed range of m_r (in AdS) by fixing $m_{(1)} \equiv 1.34 m_1$ as the ratio of ith roots of the first and second Bessel functions of the first kind.

[2] Lowering Λ_π increases the bound on m_1 significantly, such that the latter approaches the EFT scale of Λ_π.

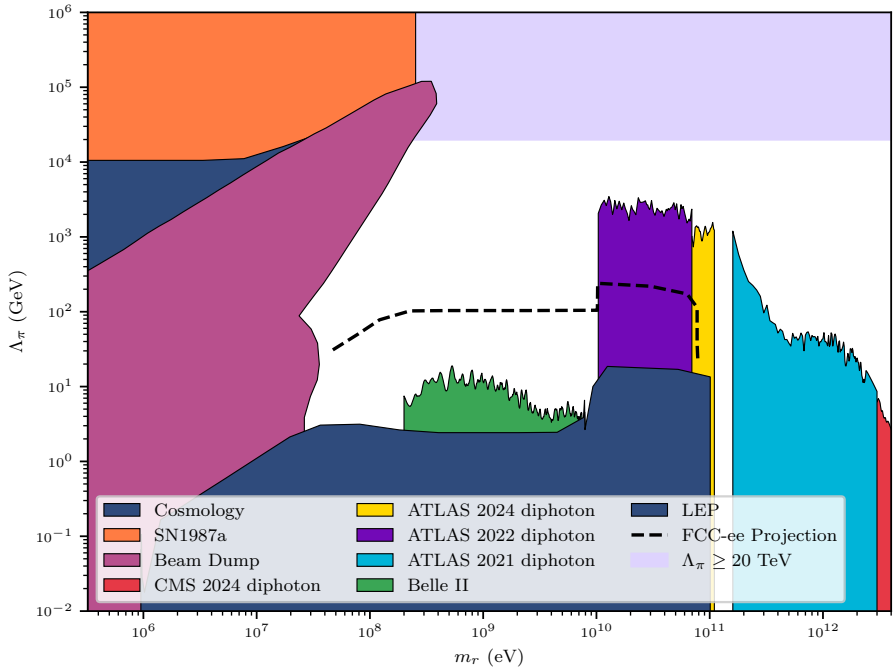

Figure 1: Experimental constraints on the radion in the (Λ_π, m_r) parameter space. The outlined shaded regions indicate exclusion limits, recast from existing bounds on pseudoscalar's diphoton coupling, as compiled in [19] and updated with [20–24]. The lavender-shaded region denotes the parameter space of interest in this work, corresponding to $\Lambda_\pi \geq 20$ TeV.

find that the aforementioned lower bound on Λ_π forces the available parameter region for the radion mass to be $m_r \geq 0.5$ GeV, where lighter radions are excluded by a combination of the following: LEP $Z \to \gamma\gamma$ decays [19], beam-dump, cosmological constraints and supernova cooling bounds from Supernova (SN) 1987a[3]. We present the parameter space of interest to this work in Figure 1.

To encode the bulk geometry, we find that the expression for the Ricci curvature

$$R(\varphi) = \frac{1}{r_c^2}\left[20(\partial_\varphi A)^2 - 8\partial_\varphi^2 A\right], \tag{10}$$

which yields

$$R(0)r_c^2 = 20\left(kr_c - \frac{\phi_1^2 ur_c}{24}\right)^2 - \frac{2}{3}\phi_1^2(ur_c)^2 \tag{11}$$

near the Planck brane. In terms of the theoretical parameters, increasing the radion mass corresponds to larger values of ur_c and/or ϕ_1, and as ϕ_1 increases, $R(0)$ switches sign from positive to negative[4]–

[3] For simplicity, we have assumed that the radion behaves similar to ALPs, with a dominant two-photon coupling governing its production and escape from the supernova core. As demonstrated by [25], stronger couplings to nucleons or electrons may lead to prompt decays being trapped within the star, relaxing and possibly reopening the SN1987A cooling constraint. However, as we will see, whether or not this region of parameter space is open is ultimately irrelevant for the present work.

[4] AdS corresponds to positive scalar curvature in our mostly minus metric convention.

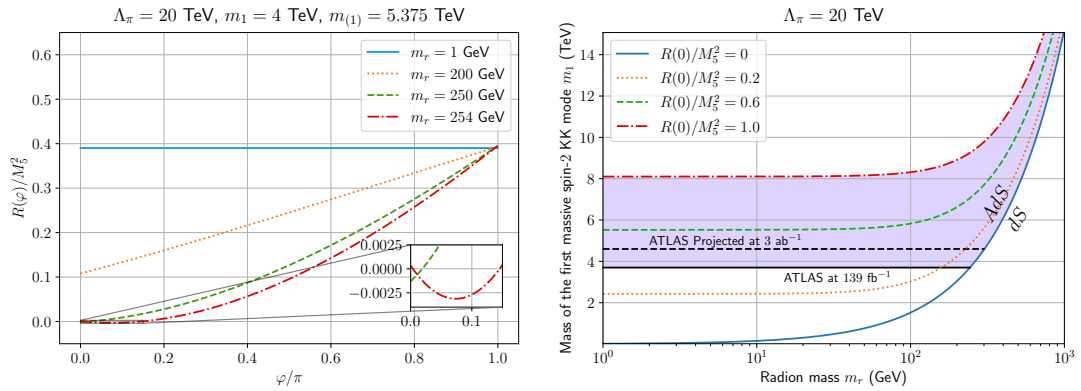

Figure 2: Left panel: Ricci curvature along the extra dimension for representative (Λ_π, m_1). For $\Lambda_\pi = 20$ TeV and $m_1 = 4$ TeV, $m_r \gtrsim 250$ GeV drives $R(0) > 0$ (locally dS) and is excluded. Right panel: Allowed region in the (m_r, m_1) plane at fixed $\Lambda_\pi = 20$ TeV, with contours of $R(0)/M_5^2$. Horizontal lines indicate current and projected diphoton limits on m_1.

that is, the space becomes locally de Sitter (and is therefore unstable to local fluctuations in energy density [26, 27]) once

$$\frac{\phi_1^2}{24} > \frac{kr_c}{ur_c}\left[1 - \sqrt{\frac{4}{5}}\left(\frac{ur_c}{kr_c}\right)^{1/2} + \cdots\right], \tag{12}$$

where requiring a large hierarchy allows us to expand the (positive) root of $\frac{\phi_1^2}{24}$ in terms of $ur_c/kr_c \ll 1$. We show this behaviour in the mini-window of Figure 2 (left panel), assuming $\Lambda_\pi = 20$ TeV and $m_1 = 4$ TeV as we increase the radion mass, such that there is an upper bound $m_r \lesssim 250$ GeV by necessitating our bulk geometry to be AdS. The allowed region in the $\{m_1, m_r\}$ plane is thus shown in Figure 2 (right panel) for $\Lambda_\pi = 20$ TeV, with contours of different values of the Ricci curvature (in units of M_5).

4. Dark sector

The KK modes couple to TeV brane's energy-momentum tensor (SM and DM) via the induced metric $\bar{G}_{\mu\nu}$. For the lightest massive states,

$$\mathcal{L} \supset \frac{\hat{h}^{(1)}_{\mu\nu}}{\Lambda_\pi} T^{\mu\nu} + \frac{e^{2A(\pi)}\gamma_0(\pi)}{\Lambda_\pi\,\psi_1(\pi)}\,\hat{r}^{(0)}\,T^\mu{}_\mu. \tag{13}$$

In the regime $m_r/m_1 \ll 1$ we find $|e^{2A(\pi)}\gamma_0(\pi)| \simeq |\psi_1(\pi)|$, so the radion couples with effective strength $\sim 1/\Lambda_\pi$ to the trace T^μ_μ. Consequently, the s-channel mediated by the radion dominates $\Phi\Phi \to$ SM thermal annihilation. Near resonance, a narrow-width approximation yields the velocity-averaged cross-section

$$\langle\sigma v\rangle \simeq \frac{\pi\sqrt{m_r^2 - 4m_\Phi^2}\,K_1(m_r/T)}{48\,\Lambda_\pi^2\,m_\Phi^4\,T\,K_2(m_\Phi/T)^2}\,v_\Phi(m_r, m_\Phi), \tag{14}$$

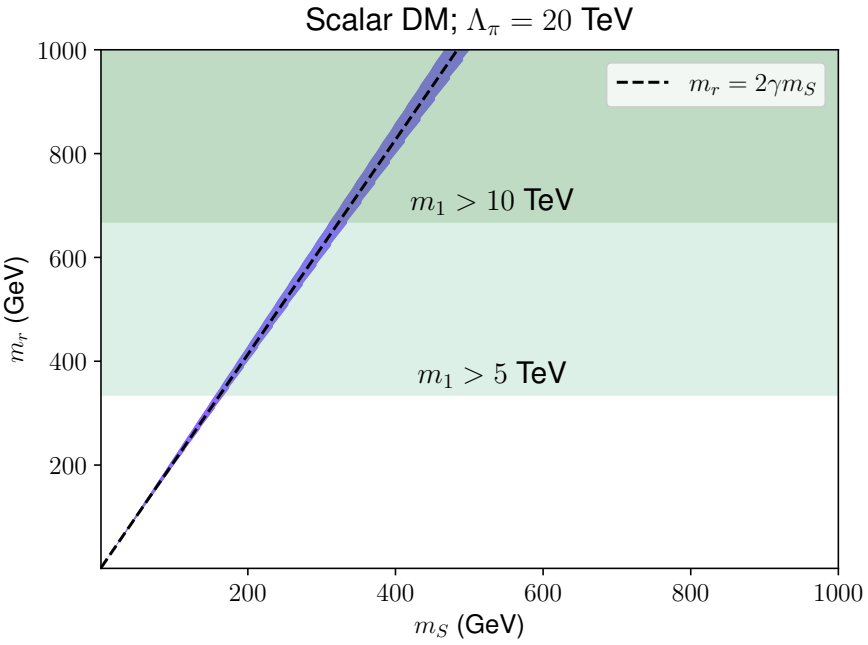

Figure 3: Scalar DM region yielding the observed relic density in (m_S, m_r) for $\Lambda_\pi = 20$ TeV. Points cluster near the thermalised on-resonance condition (dashed line) $m_r \simeq 2\gamma m_S$. Green-shaded regions are combinations of m_r and m_1 are locally AdS.

where $K_{1,2}$ are first and second modified Bessel functions of the second kind, T is temperature and DM mass m_Φ.

We consider scalar (S), vector (V), and fermion (χ) DM localised on the IR brane with mass m_Φ, and interaction-dependent factors $\upsilon_S = (m_r^2 + 2m_S^2)^2$, $\upsilon_V = \frac{1}{9}(m_r^4 - 4m_r^2 m_V^2 + 12m_V^4)$, and $\upsilon_\chi = \frac{1}{2}m_\chi^2(m_r^2 - 4m_\chi^2)$. For freezout-temperature[5] $T \simeq m_\Phi/20$ and $m_\Phi \simeq m_r/(2\gamma(v))$ near resonance we obtain the following results[6]:

$$\langle\sigma v\rangle_{SS} \approx 1.72 \times 10^{-22}\,\mathrm{cm}^3/\mathrm{s} \left(\frac{1\ \mathrm{TeV}}{\Lambda_\pi}\right)^2 \tag{15}$$

$$\langle\sigma v\rangle_{VV} \approx 6.38 \times 10^{-24}\,\mathrm{cm}^3/\mathrm{s} \left(\frac{1\ \mathrm{TeV}}{\Lambda_\pi}\right)^2 \tag{16}$$

$$\langle\sigma v\rangle_{\chi\chi} \approx 5.93 \times 10^{-25}\,\mathrm{cm}^3/\mathrm{s} \left(\frac{1\ \mathrm{TeV}}{\Lambda_\pi}\right)^2 \tag{17}$$

Matching $\Omega_{\mathrm{DM}}h^2$ (i.e. $\langle\sigma v\rangle \sim 10^{-26}\,\mathrm{cm}^3/\mathrm{s}$) for observed DM relic density [4, 28] points to viable funnels for scalar (vector) DM with $\Lambda_\pi \sim 20 - 120\,(20 - 40)$ TeV. In Figure 3, we present the viable region of parameter space for the scalar case, in the $m_r - m_S$ plane.

Note that for lower DM masses between $\simeq 5 - 80$ GeV, the resonant radion mass ($\simeq 2m_\Phi$) primarily decays to b-quarks at tree level. In this case there are stringent indirect DM bounds [29] as shown in Figure 4.

[5] T_f therefore implies relativistic (relative) velocities $v = \sqrt{16T_f/(\pi m_\Phi)}$, with corresponding Lorentz factors $\gamma(v)$.
[6] Note the helicity suppression for fermion DM near resonance $m_\chi \simeq 2m_r$.

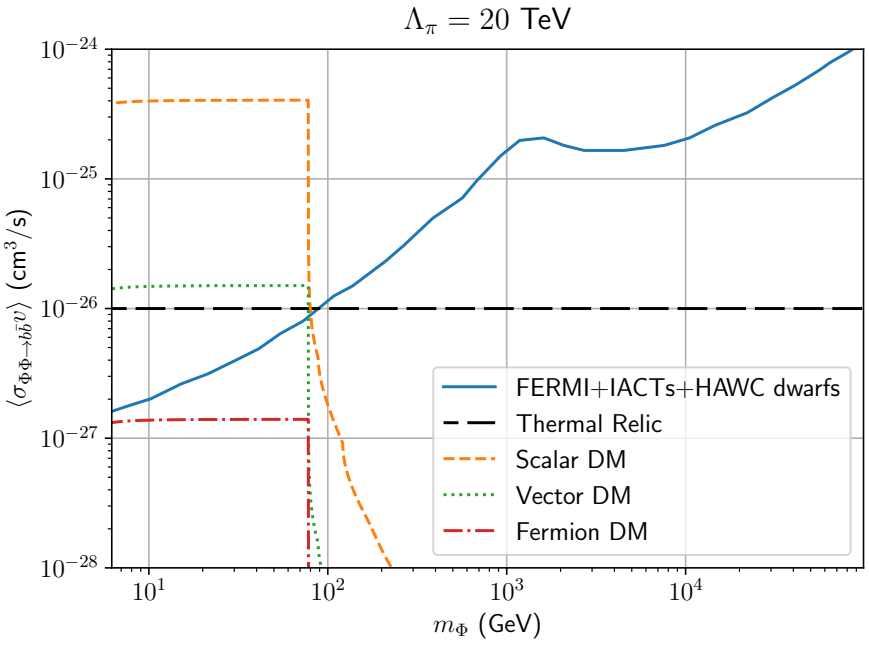

Figure 4: Indirect bounds for $r \to b\bar{b}$ compared to radion-portal predictions at $\Lambda_\pi = 20$ TeV. The range $m_{\rm DM} \in [5, 80]$ GeV is disfavored.

5. Conclusion

A stabilised RS1 model with DFGK back-reaction yields a consistent radion-portal WIMP scenario. Scalar DM achieves the relic density for $\Lambda_\pi \sim$ 20–100 TeV; vector DM is viable in a narrower resonance band of $\Lambda_\pi \sim$ 20–40 TeV; whilst fermion DM is disfavoured near resonance. Classical control enforces $m_r^{\rm max}(\Lambda_\pi; m_1)$, giving $m_r \lesssim 250$ GeV at $(\Lambda_\pi, m_1) = (20\ \text{TeV}, 4\ \text{TeV})$. Present direct detection is weak in this regime; indirect searches exclude $m_{\rm DM} \in [5, 80]$ GeV when $r \to b\bar{b}$ dominates tree level decays.

References

[1] G. Bertone and D. Hooper, *History of dark matter*, *Rev. Mod. Phys.* **90** (2018) 045002, [1605.04909].

[2] M. Cirelli, A. Strumia and J. Zupan, *Dark Matter*, 2406.01705.

[3] Planck collaboration, N. Aghanim et al., *Planck 2018 results. VI. Cosmological parameters*, *Astron. Astrophys.* **641** (2020) A6, [1807.06209].

[4] E. W. Kolb and M. S. Turner, *The Early Universe*, vol. 69. Taylor and Francis, 5, 2019, 10.1201/9780429492860.

[5] LZ Collaboration collaboration, J. Aalbers et al., *Dark Matter Search Results from 4.2 Tonne-Years of Exposure of the LUX-ZEPLIN (LZ) Experiment*, 2410.17036.

[6] I. Antoniadis, *A Possible new dimension at a few TeV*, *Phys. Lett. B* **246** (1990) 377–384.

[7] N. Arkani-Hamed, S. Dimopoulos and G. R. Dvali, *The Hierarchy problem and new dimensions at a millimeter*, *Phys. Lett. B* **429** (1998) 263–272, [hep-ph/9803315].

[8] L. Randall and R. Sundrum, *A Large mass hierarchy from a small extra dimension*, *Phys. Rev. Lett.* **83** (1999) 3370–3373, [hep-ph/9905221].

[9] L. Randall and R. Sundrum, *An Alternative to compactification*, *Phys. Rev. Lett.* **83** (1999) 4690–4693, [hep-th/9906064].

[10] W. D. Goldberger and M. B. Wise, *Modulus stabilization with bulk fields*, *Phys. Rev. Lett.* **83** (1999) 4922–4925, [hep-ph/9907447].

[11] W. D. Goldberger and M. B. Wise, *Phenomenology of a stabilized modulus*, *Phys. Lett. B* **475** (2000) 275–279, [hep-ph/9911457].

[12] O. DeWolfe, D. Z. Freedman, S. S. Gubser and A. Karch, *Modeling the fifth-dimension with scalars and gravity*, *Phys. Rev. D* **62** (2000) 046008, [hep-th/9909134].

[13] R. Sekhar Chivukula, D. Foren, K. A. Mohan, D. Sengupta and E. H. Simmons, *Scattering amplitudes of massive spin-2 Kaluza-Klein states grow only as $O(s)$*, *Phys. Rev. D* **101** (2020) 055013, [1906.11098].

[14] R. S. Chivukula, D. Foren, K. A. Mohan, D. Sengupta and E. H. Simmons, *Massive Spin-2 Scattering Amplitudes in Extra-Dimensional Theories*, *Phys. Rev. D* **101** (2020) 075013, [2002.12458].

[15] R. S. Chivukula, D. Foren, K. A. Mohan, D. Sengupta and E. H. Simmons, *Spin-2 Kaluza-Klein mode scattering in models with a massive radion*, *Phys. Rev. D* **103** (2021) 095024, [2104.08169].

[16] R. S. Chivukula, D. Foren, K. A. Mohan, D. Sengupta and E. H. Simmons, *Spin-2 Kaluza-Klein scattering in a stabilized warped background*, *Phys. Rev. D* **107** (2023) 035015, [2206.10628].

[17] C. Charmousis, R. Gregory and V. A. Rubakov, *Wave function of the radion in a brane world*, *Phys. Rev. D* **62** (2000) 067505, [hep-th/9912160].

[18] R. S. Chivukula, J. A. Gill, K. A. Mohan, G. Sanamyan, D. Sengupta, E. H. Simmons et al., *Limits on Kaluza-Klein Portal Dark Matter Models*, 2411.02509.

[19] J. Jaeckel and M. Spannowsky, *Probing MeV to 90 GeV axion-like particles with LEP and LHC*, *Phys. Lett. B* **753** (2016) 482–487, [1509.00476].

[20] Belle-II collaboration, F. Abudinén et al., *Search for Axion-Like Particles produced in e^+e^- collisions at Belle II*, *Phys. Rev. Lett.* **125** (2020) 161806, [2007.13071].

[21] ATLAS collaboration, G. Aad et al., *Search for resonances decaying into photon pairs in 139 fb^{-1} of pp collisions at $\sqrt{s}$=13 TeV with the ATLAS detector*, *Phys. Lett. B* **822** (2021) 136651, [2102.13405].

[22] ATLAS collaboration, G. Aad et al., *Search for boosted diphoton resonances in the 10 to 70 GeV mass range using 138 fb^{-1} of 13 TeV pp collisions with the ATLAS detector*, *JHEP* **07** (2023) 155, [2211.04172].

[23] ATLAS collaboration, G. Aad et al., *Search for diphoton resonances in the 66 to 110 GeV mass range using pp collisions at $\sqrt{s}$ = 13 TeV with the ATLAS detector*, *JHEP* **01** (2025) 053, [2407.07546].

[24] CMS collaboration, A. Hayrapetyan et al., *Search for new physics in high-mass diphoton events from proton-proton collisions at $\sqrt{s}$ = 13 TeV*, *JHEP* **08** (2024) 215, [2405.09320].

[25] F. Abu-Ajamieh, J. S. Lee and J. Terning, *The Light Radion Window*, *JHEP* **10** (2018) 050, [1711.02697].

[26] J. D. Barrow, *The Deflationary Universe: An Instability of the De Sitter Universe*, *Phys. Lett. B* **180** (1986) 335–339.

[27] T. Padmanabhan, *Cosmological constant: The Weight of the vacuum*, *Phys. Rept.* **380** (2003) 235–320, [hep-th/0212290].

[28] S. Dodelson, *Modern Cosmology*. Academic Press, Amsterdam, 2003.

[29] Hess, HAWC, VERITAS, MAGIC, H.E.S.S., Fermi-LAT collaboration, H. Abdalla et al., *Combined dark matter searches towards dwarf spheroidal galaxies with Fermi-LAT, HAWC, H.E.S.S., MAGIC, and VERITAS*, *PoS* **ICRC2021** (2021) 528, [2108.13646].